International Journal of Scientific Research in Science and Technology
Print ISSN: 2395-6011 | Online ISSN: 2395-602X (www.ijsrst.com)
doi : https://doi.org/10.32628/IJSRST52310237

Implementation of Standard Deviation Map (SDM) for an Automation of Spatial Resolution Measurements on Computed Tomography Images of ACR CT Accreditation Phantom

Didik Rahmadi [1] , Choirul Anam [1,*] , Eko Hidayanyo [1] , Ariij Naufal [1]

[1]Department of Physics, Faculty of Sciences and Mathematics, Diponegoro University, Jl. Prof Soedarto SH, Tembalang, Semarang, Central Java, Indonesia

* Corresponding author: anam@fisika.fsm.undip.ac.id

ARTICLEINFO

Article History:

Accepted: 05 March 2023
Published: 22 March 2023

Publication Issue
Volume 10, Issue 2
March-April-2023

Page Number
256-262

ABSTRACT

This study is to develop an automated method to determine the spatial resolution of computed tomography (CT) images on line-pair objects of the American College of Radiology (ACR) CT accreditation phantom. The ACR phantom was scanned using a GE Healthcare 128-slice CT scanner with seven different reconstruction filters of E1, E2, E3, LU, S1, S2, S3. The automated method involved building a standard deviation map (SDM), segmenting the line-pair objects within SDM images, determining the region of interest (ROI) within line pair object, and determining a resolvable line-pair object with dynamic threshold which is dependent on image noise. The scanning parameters were fixed at 120 kVp and 160 mAs. The results of automated method were compared with those from manual measurements performed by five human observers. The automatic method produced spatial resolution results of 0.7, 0.7, 0.7, 0.7, 0.6, 0.6, and 0.6 lp/mm for filters E1, E2, E3, LU, S1, S2, and S3, respectively, while the manual measurements yielded results of 0.6, 0.6, 0.6, 0.7, 0.6, 0.5, and 0.5 lp/mm. The differences between the manual and automatic measurement results were small, with a maximum difference of 0.1 lp/mm. Hence, the automatic measurement of spatial resolution on line-pair objects of the ACR CT accreditation phantom is a feasible and reliable method.

Keywords: CT scanner, ACR CT accreditation phantom, reconstruction filter, automatic, spatial resolution

I. INTRODUCTION

Computed tomography (CT) is an imaging modality commonly and widely used clinically (Chokami et al., 2020). In CT practice, acceptable image quality of CT should be achieved with low radiation dose (Sanders et al., 2016). Therefore, many advanced techniques to obtain good quality images have developed, such as iterative reconstruction (IR) technique, tube current modulation (TCM) technique, and so on (Solomon et al., 2020, Christianson et.al, 2015). Good image quality is characterized by several parameters, one of which is spatial resolution (Goldman et al., 2007, Love et al., 2013, Anam et al., 2018).

Spatial resolution refers to ability of an imaging system to distinguish small objects that are close together (Brüllmann and Schulze, 2015; Bushberg et al, 2020). Every object in the image is blurred so that if there are two small objects that are close together at a very close distance, then they may appear as one object because the two objects are overlapping each other. Practically, spatial resolution of the image can be identified from the last resolvable number of line-pair objects separated at a certain distance in centimeters or millimeters. The last line-pair object is observed by visual observation of white lines (line-pairs) on a black background (Bushong, 2020; Seeram, 2016; Staude et al., 2011). It is important to note that visual observation on the last resolvable line-pairs object is observer-dependent (Gopal, 2009).

Droege and Morin have developed a method of measuring spatial resolution numerically by making region of interest (ROI) on line-pair objects to get the response and reconstructed a curve of modulation transfer function (MTF) from them (Droege and Morin, 1982). It is noted that MTF curve is an acceptable comprehensive representation of spatial resolution of an image. MTF is usually obtained from point spread function (PSF), line-spread function (LSF), or edge-spread function (ESF), and not from line-pairs object. Therefore, the work of Droege and Morin is important contribution for providing an alternative approach to obtain MTF curve. However, the proposed method by Droege and Morin is still carried out manually so it may not impractical in routine quality assurance (QA) procedures, especially in busy medical centers. Hence, we developed a new alternative algorithm for automated method for measuring spatial resolution on line-pair object to overcome weaknesses of manual method. In this regard, we employed recent technique in CT image processing, i.e. standard deviation map (SDM) described in AAPM TG 233 (AAPM). Therefore, the purpose of this study is to automatically measure the spatial resolution of CT images on line-pair objects of ACR CT accreditation phantom using the SDM.

II. METHODS AND MATERIAL

A. Phantom images

We used spatial resolution module of the ACR CT accreditation phantom. This module consists of eight line-pair objects with sizes of 0.4, 0.5, 0.6, 0.7, 0.8, 0.9, 1.0 and 1.2 lp/mm. Image samples of the module are shown in Figure 1. Window-width (WW) and window-level (WL) at 100 and 1100 Hounsfield unit (HU) are recommended for visual observation of line pairs [15,16] (Figure 1b). We scanned the phantom with a GE Revolution EVO 128-slice CT scanner with input parameters shown in Table 1. The images were stored in Digital Imaging and Communications in Medicine (DICOM) format. Image samples with various reconstruction filters are shown in Figure 2.

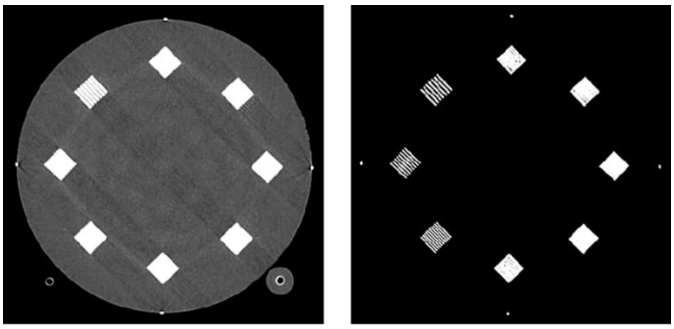

(a) (b)

Figure 1. Image sample of ACR CT Accreditation phantom displayed with two different windows: (a) with soft tissue window, and (b) with window-width (WW) of 100 HU and window-level (WL) of 1100 HU.

Table 1. CT input parameters in this study

Parameters	Value
Scan type	Helical
Convolution kernels	Standard
Revolution time	0.8 seconds
Tube current	160 mA
Tube voltage	120 kV
Slice thickness	1.25 mm
Field of view	211 mm
Pitch	0.531
Reconstruction filter	E1, E2, E3, LU, S1, S2, S3

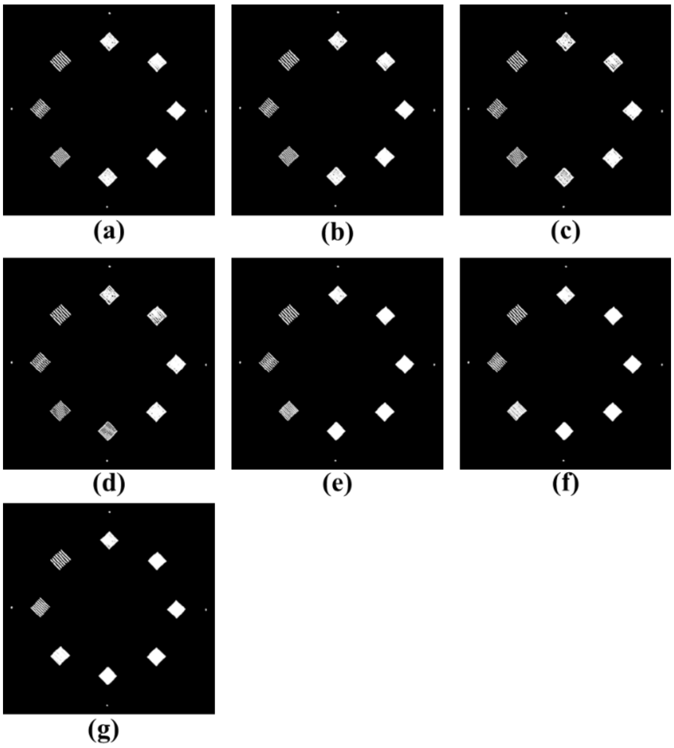

Figure 2. Image samples of ACR CT Accreditation phantom reconstructed with various reconstruction filters: (a) E1, (b) E2, (c) E3, (d) LU, (e) S1, (f) S2, and (g) S3.

B. Automatic Spatial Resolution Measurement

We proposed a new algorithm for automatic spatial resolution measurement on the line-pair object of ACT CT accreditation phantom. The automatic measurement for spatial resolution in this study was integrated to the software IndoQCT [17]. The graphical user interface (GUI) for automatic measurement of spatial resolution is shown in Figure 3.

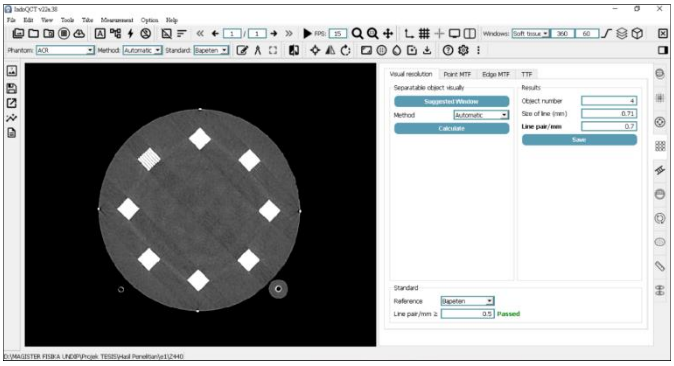

Figure 3. Graphical user interface (GUI) automatic measurement of spatial resolution

The main idea for automatic spatial resolution measurement on the line-pair objects is by using a SDM. This method was started with opening the original image (Fig. 4a). The original image was then converted to SDM [18]. The conversion is carried out with a 3 × 3 pixels of sliding window to calculate the SD at each pixel location within the image. This process changed the image in HU to an SDM displayed with a hot colormap (Fig. 4b). In this SDN, the pixels that appear brighter indicate a higher SD. After that, detection of the line-pair object was performed by segmentation on the SDM with a threshold of 20 HU (Fig. 4c) and erosion on the binary image with the purpose of eliminating small objects. This process produced a binary image that contains line-pair objects and free of artifacts (Fig. 4d). To detect all line–pair objects and avoid hollows in line-pair objects, the holes in the line-pairs objects were filled (Fig. 4e). Centroids of each line-pair object were then determined with equation (1).

$$x_{cen}, y_{cen}) = \frac{1}{N}\sum_{i=1}^{N}(x_i, y_i) \qquad (1)$$

Circle ROIs with adjusted radius were then placed on the SDM based on each centroid coordinate of line pairs (Fig. 4f). The average values of SD were taken from inside the ROI.

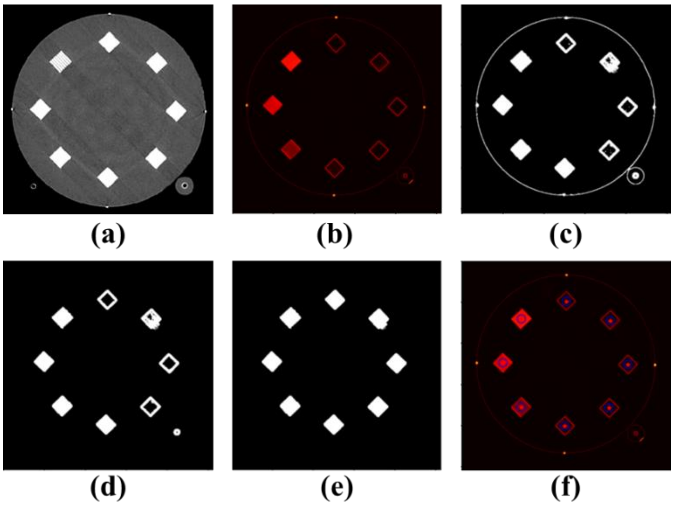

Figure 4. Steps of automatic spatial resolution measurement on line-pair object: (a) original image, (b) standard deviation map (SDM) with hot colormap, (c) binary image obtained with threshold of 20 HU, (d) eroded binary image, (e) hollow line-pair objects is filled, (f) circular region of interests (ROIs) placed on each line-pair object of SDM.

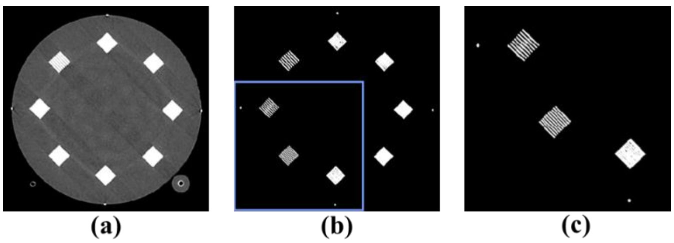

Figure 5. Images for manual observation: (a) Image with soft tissue window, (b) image with window-width (WW) of 100 HU and window-level (WL) of 1100 HU, and (c) zoomed-in image.

The last resolvable line-pair object was calculated with a certain dynamic threshold depending on the image noise, as shown in Equation (2).

$$threshold = \frac{(25 \times SD_{max})}{300} \qquad (2)$$

This threshold corresponds to the last resolvable line-pair object that can still be distinguished by human observation.

C. Human observer

The manual measurement was determined by five human observers. This method was carried out on images with recommended window settings to increase line-pair visibility (Fig. 5b). Furthermore, the image was zoomed-in to make the line-pair object to be clearer for observers (Fig. 5c). The observers selected the last resolvable line-pair object based on their subjectivities. The method was applied to all reconstruction filters (i.e. E1, E2, E3, LU, S1, S2, and S3). Results from five human observers were averaged to obtain one value of spatial resolution.

III. RESULTS AND DISCUSSION

Figure 6 shows six SDMs of the spatial resolution module of the ACR CT accreditation phantom and ROIs located within the lair-pair objects. It is seen that our software accurately locates the ROIs automatically for all reconstruction filters of E1, E2, E3, LU, S1, S2, and S3. The results of the automatic and manual measurements of spatial resolution are tabulated in Table 2. It appears that all spatial resolution values are greater than 0.5 lp/mm, which is fairly good for image with matrix size of 512 × 512. It is found that automatic method tends to produce greater spatial resolution than from manual observation, with maximum difference between both is 0.1 lp/mm.

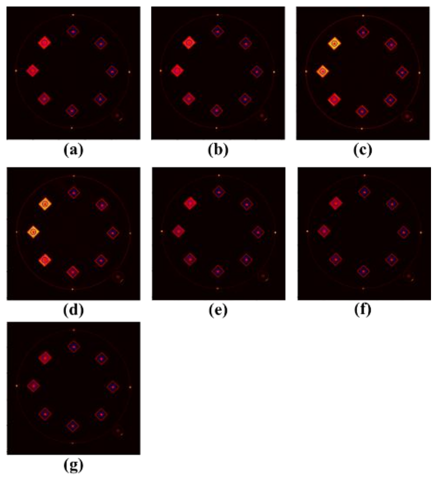

Figure 6. SDMs of the spatial resolution module of the ACR CT accreditation phantom and locations of ROIs within the lair-pair objects for various reconstruction filters: (a) E1, (b) E2, (c) E3, (d) LU, (e) S1, (f) S2, and (g) S3.

Table 2. Comparison of the results of spatial resolution measurements between automatic and manual measurements on the ACR CT accreditation phantom.

Reconstruction filter	Noise (HU)	Measurements of spatial resolution (lp/mm)		Difference (lp/mm)
		Automatic	Manual	
	Mean ± SD	Mean ± SD	Mean ± SD	
E1	9.1 ± 0.3	0.7 ± 0.0	0.6 ± 0.0	0.1
E2	9.7 ± 0.4	0.7 ± 0.0	0.6 ± 0.0	0.1
E3	14.6 ± 0.6	0.7 ± 0.0	0.6 ± 0.0	0.1
LU	15.3 ± 0.6	0.7 ± 0.0	0.7 ± 0.0	0.0
S1	7.3 ± 0.3	0.6 ± 0.0	0.6 ± 0.0	0.0
S2	6.8 ± 0.3	0.6 ± 0.0	0.5 ± 0.0	0.1
S3	6.4 ± 0.2	0.6 ± 0.0	0.5 ± 0.0	0.1

This study aimed at development of an automated method for measuring spatial resolution using line-pair object of the American College of Radiology (ACR) CT accreditation phantom and to evaluate its performance on various reconstruction filters. The reconstruction filters used in this study were categorized into three groups: edge filters (E1, E2, E3), lung filters (LU), and smoothing filters (S1, S2, S3).

The results of this study showed that results of the automated measurements are comparable to those from human observations. The maximum discrepancy between both is only 0.1 lp/mm, with results of automatic method tends to be greater than those from manual observations. This indicates that the manual measurement of the last resolvable line-pair object is perceived similarly to the human eye. Although individual observations may produce slightly different results, the average calculated spatial resolution is expected to be close to the automatic measurement.

Our method relies on the standard deviation map (SDM) which is influenced by image noise. Therefore, testing the method on various types of reconstruction filters is essential. Reconstruction filters have their own unique characteristics noise level, noise texture, spatial resolution. In addition, the reconstruction can cause some artifacts and impact the resulted images. However, morphological operations such as erosion and dilation can be used to overcome these artifacts that may disturb an automatic spatial resolution measurement. Additionally, some filters can shift the CT number of the line pair forming material, resulting in variations in the SDM and incorrect counting of line pair objects. An adaptive dynamic threshold to image noise is a promising approach to address this problem. Nonetheless, the effect of artifacts other than those in the images used in this study is still unknown. Therefore, it is recommended to measure a spatial resolution from images with minimal artifacts. The results demonstrated that edge and lung filters produced the highest spatial resolution value of 0.7 lp/mm, while the smoothing filter had the lowest spatial resolution value of 0.6 lp/mm. This indicates that reconstruction filters of edge and lung filters have a greater spatial resolution than smooth filters [19,20]. Table 2 shows the spatial resolutions for each reconstruction filter, providing useful information for researchers and practitioners in selecting an appropriate filter for their specific needs.

The developed automatic method provides a reliable and efficient method for measuring the spatial resolution of CT images using the line-pair object of the ACR phantom. However, testing the developed method on other parameters, such as various tube current, tube voltage, pitch, slice thickness, does not carry out yet. In addition, the method has been tested on images from one CT scanner. Therefore, comprehensive evaluations of the method should be carried out in the next studies.

IV. CONCLUSION

In conclusion, an automated method for measuring spatial resolution in CT images using the line-pair objects of the ACR phantom has been successfully developed. The automatic method runs well for various reconstruction filters. Results of the automatic measurements are comparable to the manual measurements, with only small difference of 0.1 lp/mm. We also observed that the software is robust against artifacts in images produced by different reconstruction filters.

V. ACKNOWLEDGMENTS

This work was funded by the World Class Research University (WCRU), Diponegoro University, No. 118-08/UN7.6.1/PP/2021.

VI. REFERENCES

[1]. Chokami HK, Hosseini SA, Ghorbanzadeh M, Mohammadi M. QCT: A measuring tool dedicated to the estimation of image parameters for quality assurance/quality control programs of CT scanners. 2020 IEEE International Symposium on Medical Measurements and Applications (MeMeA). 2020; 1-6.

[2]. Sanders J, Hurwitz L, Samei E. Patient-specific quantification of image quality: An automated method for measuring spatial resolution in clinical CT images. Medical Physics. 2016; 43(10): 5330-5338.

[3]. Solomon J, Lyu P, Marin D, Samei E. Noise and spatial resolution properties of a commercially available deep learning-based CT reconstruction algorithm. Medical Physics. 2020; 47(9): 3961-3971.

[4]. Christianson O, Winslow J, Frush DP, Samei E. Automated technique to measure noise in clinical CT examinations. American Journal of Roentgenology. 2015; 205(1): W93–W99.

[5]. Goldman LW. Principles of CT: radiation dose and image quality. Journal of Nuclear Medicine Technology. 2007 Dec;35(4): 213-25.

[6]. Love A, Olsson ML, Siemund R, et al. Six iterative reconstruction algorithms in brain CT: a phantom study on image quality at different radiation dose levels. British Journal of Radiology. 2013;86: 20130388.

[7]. Anam C, Fujibuchi T, Budi WS, Haryanto F, Dougherty G. An algorithm for automated modulation transfer function measurement using an edge of a PMMA phantom: Impact of field of view on spatial resolution of CT images. Journal of Applied Clinical. Medical Physics. 2018; 19(6): 244–252.

[8]. Brüllmann D, Schulze RK. Spatial resolution in CBCT machines for dental/maxillofacial applications-what do we know today?. Dentomaxillofacial Radiology. 2015;44(1): 20140204.

[9]. Mahesh M. The Essential Physics of Medical Imaging, Third Edition. Medical Physics. 2013 Jul;40(7) :28524933.

[10]. Bushong, Stewart C. Radiologic science for technologists e-book: physics, biology, and protection. Elsevier Health Sciences, 2020.

[11]. Seeram, Euclid. Computed Tomography-E-Book: Physical Principles, Clinical Applications, and Quality Control. Elsevier Health Sciences, 2015.

[12]. Staude A, Goebbels J. Determining the spatial resolution in computed tomography comparison

of MTF and line-pair structures. International Symposium on Digital Industrial Radiology and Computed Tomography. 2011; 16(11).
[13].Gopal A, Samant SS. Use of a line-pair resolution phantom for comprehensive quality assurance of electronic portal imaging devices based on fundamental imaging metrics. Medical Physics. 2009;36(6): 2006-2015.
[14].Droege RT, Morin RL. A practical method to measure the MTF of CT scanners. Medical Physics. 1982;9(5): 758–60.
[15].McCollough CH, Bruesewitz MR, McNitt-Gray MF, et al. American College of Radiology. The phantom portion of the American College of Radiology (ACR) computed tomography (CT) accreditation program: practical tips, artifact examples, and pitfalls to avoid. Medical Physics. 2004 Sep;31(9): 2423-42.
[16].Cropp RJ, Seslija P, Tso D, Thakur Y. Scanner and kVp dependence of measured CT numbers in the ACR CT phantom. Journal of Applied Clinical Medical Physics. 2013; 14 (6): 338-349.
[17].Anam C, Naufal A, Fujibuchi T, Matsubara K, Dougherty G. Automated development of the contrast-detail curve based on statistical low-contrast detectability in CT images. Journal of Applied Clinical Medical Physics. 2022;23(9): e13719.
[18].Anam C, Arif I, Haryanto F. An improved method of automated noise measurement system in CT images. Journal of Biomedical Physics and Engineering. 2021;11(2): 163-174.
[19].Seung-Wan Lee, Chang-Lae Lee, Hyo-Min Cho, Hye-Suk Park, Dae-Hong Kim, Yu-Na Choi and Hee-Joung Kim. Effects of reconstruction parameters on image noise and spatial resolution in cone-beam computed tomography. Journal of the Korean Physical Society. 2011; 59 (4): 2825-2832.
[20].Rueckel J, Stockmar M, Pfeiffer F & Herzen J. Spatial resolution characterization of an X-ray microCT system. Applied Radiation and Isotopes. 2014;94, 230-234.

Cite this article as :

Didik Rahmadi, Choirul Anam, Eko Hidayanyo, Ariij Naufal, "Implementation of Standard Deviation Map (SDM) for an Automation of Spatial Resolution Measurements on Computed Tomography Images of ACR CT Accreditation Phantom", International Journal of Scientific Research in Science and Technology (IJSRST), Online ISSN : 2395-602X, Print ISSN : 2395-6011, Volume 10 Issue 2, pp. 256-262, March-April 2023. Available at doi : https://doi.org/10.32628/IJSRST52310237
Journal URL : https://ijsrst.com/IJSRST52310237